Marine and Petroleum Geology 91 (2018) 470–479

Contents lists available at ScienceDirect

Marine and Petroleum Geology

journal homepage: www.elsevier.com/locate/marpetgeo

Research paper

Significance of stable carbon isotope trends in carbonate concretions formed in association with anaerobic oxidation of methane (AOM), Middle and Upper Devonian shale succession, western New York State, USA

Gary G. Lash

Department of Geology and Environmental Sciences, State University of New York – Fredonia, Fredonia, NY, 14063, USA

ARTICLE INFO

Keywords:
Concretions
Carbon isotopes
Sulfate
Anaerobic oxidation of methane
Carbon dioxide reduction

ABSTRACT

Carbonate concretions are concentrated along discrete stratigraphic horizons within Middle and Upper Devonian carbonaceous black and organic-deficient gray shale of western New York State. Textural characteristics preserved throughout studied concretions, including a clay grain microfabric typical of flocculated clay and spherical algal cysts, are consistent with a model entailing the formation of low-density, compaction-resistant calcium carbonate masses at shallow burial depth, within the zone of bacterial sulfate reduction. Burial of nascent concretions to the sulfate methane transition zone (SMTZ) was accompanied by the nearly complete infilling of porosity, the diagenetic consequence of the anaerobic oxidation of methane (AOM). Each concretionary horizon, then, defines the position of the SMTZ stabilized during an episode of reduced sedimentation rate. Most analyzed concretions (75%) of the Middle Devonian Marcellus Formation into the Upper Devonian Gowanda Formation display center-to-edge profiles of increasing bulk $\delta^{13}C$; far fewer concretions are characterized by radial profiles of decreasing $\delta^{13}C$. The common radial profiles of increasing $\delta^{13}C$ can be attributed to AOM-related kinetic carbon isotope fractionation under diagenetic conditions of limited methane, which favors the production of dissolved inorganic carbon of increasing $\delta^{13}C$. Less common concretions displaying center-to-edge profiles of diminishing $\delta^{13}C$ may record the anaerobic oxidation of more strongly ^{13}C-depleted methane produced by carbon dioxide reduction, methanogenesis related to the degradation of organic matter within and near the SMTZ, or AOM back flux, an enzyme-mediated equilibrium isotope effect. These processes are favored by sulfate-limited diagenetic conditions more typical of the lower SMTZ and immediately underlying upper methanogenic zone (MEZ). Contradictory isotope profiles of texturally similar concretions can be accounted for by diagenesis associated with an extended SMTZ (ESMTZ) comprising the methane-limited SMTZ and the underlying sulfate-deficient upper MEZ. Vertical shifts of the diagenetic horizons of the ESMTZ induced by variable methane flux would have juxtaposed concretions displaying seemingly incompatible isotopic histories.

1. Introduction

Carbonate concretions, perhaps the most obvious diagenetic feature of shale and mudstone deposits of various ages, provide insight regarding the sources of carbonate cement and the nature and timing of depth-related microbial processes that affected the host shale during compaction and early diagenesis (e.g., Raiswell, 1971, 1987, 1988; Curtis et al., 1972; Hudson and Friedman, 1976; Irwin et al., 1977; Hudson, 1978; Coleman and Raiswell, 1981; Gautier and Claypool, 1984; Astin and Scotchman, 1988; Scotchman, 1991; Raiswell and Fisher, 2000, 2004; Day-Stirrat et al., 2008; Gaines and Vorhies, 2016). In particular, center-to-edge or radial bulk stable carbon isotope profiles of the calcite matrix of carbonate concretions preserve the record of evolving pore water composition during the burial history of the sediment column (Hudson and Friedman, 1976; Hudson, 1978; Coleman and Raiswell, 1981; Dix and Mullins, 1987; Astin and Scotchman, 1988; Mozley, 1989; Thyne and Boles, 1989; Coniglio and Cameron, 1990; Scotchman, 1991; Jordan et al., 1992; Mozley and Burns, 1993; Bojanowski and Clarkson, 2012; Plet et al., 2016; Gaines and Vorhies, 2016).

Carbonate concretions are concentrated along numerous 1- to 2-m-thick stratigraphic horizons throughout the Middle and Upper Devonian shale succession of western New York State. Previous investigations have related concretion formation to the anaerobic oxidation of methane (AOM) focused along discrete stratal horizons during repeated pauses of sedimentation (Lash and Blood, 2004a; Lash, 2015a, 2015b). The present paper, building on earlier work, addresses the significance of radial profiles of increasing and decreasing bulk $\delta^{13}C$ displayed by

E-mail address: Lash@fredonia.edu.

https://doi.org/10.1016/j.marpetgeo.2018.01.032
Received 14 September 2017; Received in revised form 21 January 2018; Accepted 24 January 2018

concretions recovered from throughout the shale succession, some from the same stratigraphic level. Published discussions of concretion formation have ascribed center-to-edge geochemical trends to burial-related passage of host sediment from a diagenetic environment of bacterial sulfate reduction to one dominated by methanogenesis (e.g., Jordan et al., 1992). Others have attributed such trends to the evolution over time of methane and dissolved inorganic carbon (DIC) produced within the methanogenic zone (MEZ) (Raiswell, 1987). Textural features of the studied Middle and Upper Devonian concretions suggest that they formed in association with AOM at shallow burial depth (Lash and Blood, 2004a; Lash, 2015a, 2015b). The case is made that contrasting center-to-edge isotope gradients are more consistent with what is known of the complex nature of carbon cycling associated with AOM rather than variations in the isotopic composition of deeper-sourced commingled DIC and methane.

Previous investigations of Devonian carbonate concretions of the Appalachian Basin have revealed their generally ^{18}O-depleted nature (Dix and Mullins, 1987; Criss et al., 1988; Coniglio and Cameron, 1990; Lash and Blood, 2004a). Abnormally high calculated equilibration paleotemperatures of concretions based on their depleted $\delta^{18}O$ values are contrary to field and textural observations suggesting shallow depths of carbonate precipitation (Dix and Mullins, 1987; Lash and Blood, 2004a). This apparent depth disparity has been attributed to the thermally induced diagenetic alteration of stable oxygen isotope values (Dix and Mullins, 1987; Lash and Blood, 2004a), an interpretation consistent with the premise that stable carbon isotopes are less sensitive to temperature-induced fractionation (Veizer, 1983; Gautier and Claypool, 1984). As such, the present study considers only stable carbon isotopes as they likely record a more robust history of pore fluid composition.

2. Geological framework and carbonate concretions

The Middle and Upper Devonian clastic succession of western New York State is part of an eastward-thickening body of marine shale and scattered siltstone beds that grades upward and eastward into shallow marine or brackish-water deposits (Friedman and Johnson, 1966; Woodrow et al., 1973; Baird and Lash, 1990). The shale-dominated marine deposits cropping out along the Lake Erie shoreline and in creeks of western New York are arranged in several cycles, each one defined at its base by a black shale unit that passes upward into gray shale, occasional siltstone beds, and thin black shale beds (Fig. 1A). Calcium carbonate concretions are common throughout the entire marine shale succession, occurring in both gray and black shale, from the Marcellus Formation up-section well into the Gowanda Formation (Fig. 1A).

Carbonate concretions analyzed for this study were collected from 19 laterally persistent concretion-rich horizons of the Middle Devonian Marcellus Formation upward into the Upper Devonian Gowanda Formation (Fig. 1A and B and 2A). Concretions are typically oblate ellipsoids and oriented with maximum dimensions parallel to bedding (Fig. 2B and C). Elongate concretionary masses, occasionally extending along the outcrop for more than 5 m, can be observed locally (Fig. 2C). Some larger concretions formed by the coalescence of multiple smaller concretions (Fig. 2D). Coalesced concretions were not sampled as part of the present study. Septarian fractures, observed in approximately half the studied concretions, extend outward from concretion centers, narrowing to termination at or near concretion margins. Concretions hosted by black shale reveal laminae displaying consistent thickness across the carbonate mass (Fig. 2B,E). Concretions hosted by gray shale, however, lack similar features though faint parallel laminae are occasionally observed.

3. Methods

Twenty-four concretions from 19 concretionary horizons hosted by black and gray shale were sampled for the present study (Fig. 1A; Table 1). Sampled concretions range from 14 cm to more than a meter in the longest dimension (Table 1). Samples of the microcrystalline matrix of concretions were collected along layer-parallel center-to-edge and edge-to-edge transects using a rock corer that yielded 2- to 3-cm -long rock plugs. Only those concretions that had been cleaved through their centers by natural fracturing were sampled. Two sets of three closely spaced concretions (i.e., within 2 m of each other) were sampled from two horizons within the organic-rich Rhinestreet Formation (set 1: RST1, RSTA, UC; set 2: C1, C2, EMC29; Fig. 1A; Table 1). The greatest number of concretions was sampled from the Rhinestreet Formation, including gray shale intervals (Table 1).

Calcium concentrations of concretion samples were measured by use of the NITON XL3t GOLDD handheld EDXRF (energy dispersive X-ray fluorescence) spectrometer equipped with a silicon drift detector for enhanced light element analysis. Samples were analyzed on a hands-free test stand to which the analyzer was attached. Determination of optimal exposure time was addressed by Lash and Blood (2014) and Lash (2015a,b). Samples of the present study were analyzed at the following exposure times: (1) main filter = 85 s; (2) low filter = 60 s; (3) high filter = 30 s; and (4) light filter = 170 s. Data quality was monitored in two ways during the analytical phase of the study. First, a set of certified powdered samples used as standards, including U.S.G.S. standards SGR-1 (Green River Shale), SBC-1 (Brush Creek Shale), and COQ-1 (carbonatite), were analyzed at the beginning of each data collection session. In every case, test results fell well within certified acceptable error ranges for Ca. The second method of assessing data quality addressed instrument drift. For every six samples analyzed, a standard sample was tested eight times. The reproducibility of Ca measurements was found to be within ± 7% of the standard concentration.

Stable carbon ($\delta^{13}C$) isotope analysis was carried out on calcium carbonate concretion samples by continuous flow – isotope ratio mass spectrometry at Iso-Analytical Limited, Crewe, UK, using an ANCA-G gas purification module and 20-20 mass spectrometer (Europa Scientific Ltd, Crewe, UK). Powdered concretion samples as well as reference and control carbonates were weighed in Exetainer tubes (Labco, UK), flushed with 99.995% helium, and converted to carbon dioxide by injecting phosphoric acid. Analyzed control sample material included IA-R022 (Iso-Analytical working standard calcium carbonate), NBS-18 (carbonatite), and NBS-19 (limestone). Duplicate analyses were performed on every fourth analysis. Results are reported relative to the Vienna-Pee Dee Belemnite (V-PDB) standard.

The micro-texture of matrix carbonate was analyzed by scanning electron microscopy (SEM). Approximately half of the concretion samples selected for SEM examination were etched with dilute HCl in order to examine the nature of the clay grain microfabric preserved by precipitation of authigenic carbonate. Host shale samples were prepared following the methodology of O'Brien and Slatt (1990). Concretion and shale samples were mounted on double-sided adhesive carbon tape and analyzed on a Phenom ProX SEM equipped with an energy dispersive spectroscopy (EDS) detector operating at acceleration voltages of between 5 and 15 keV.

4. Carbonate concretions – record of anaerobic oxidation of methane

Stratally confined carbonate concretions hosted by Upper Devonian shale of western New York State are interpreted to have formed in association with AOM and consequent enhanced alkalinity (Lash and Blood, 2004a,b; Lash, 2015a,b). Each concretionary horizon is interpreted to reflect the diagenetic signature of AOM within the sulfate methane transition zone (SMTZ), a diagenetic horizon of indeterminate thickness along which downward-diffusing seawater sulfate and upward-diffusing methane are consumed by a consortium of methane-oxidizing archea and sulfate-reducing bacteria (Reeburgh, 1976; Hoehler et al., 1994; Niewöhner et al., 1998; Hinrichs et al., 1999;

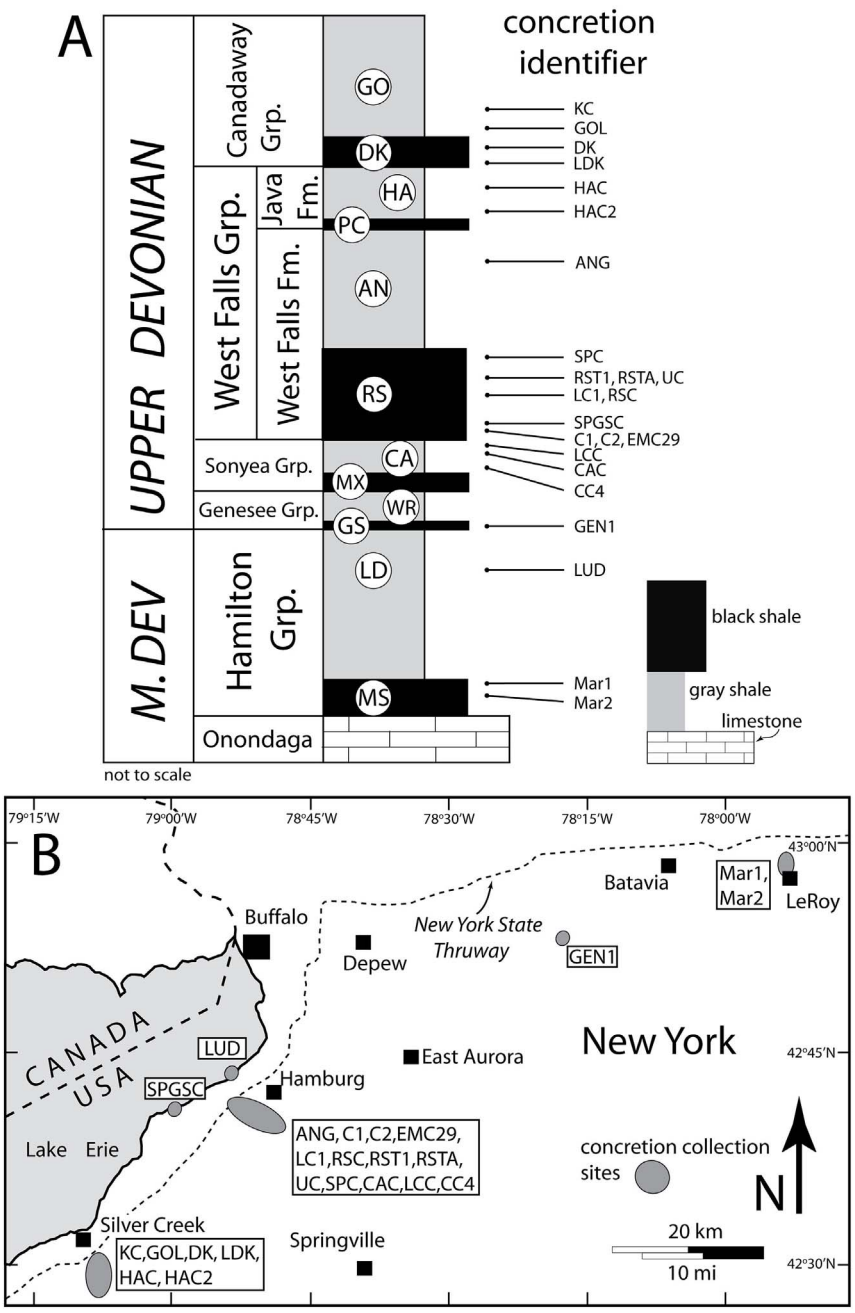

Fig. 1. (A) Generalized Middle and Upper Devonian stratigraphy of the western New York State region of the Appalachian Basin showing approximate stratigraphic positions of carbonate concretions analyzed in the present study. Circled upper case letters on the stratigaphic column refer to formal rock units: MS = Marcellus Formation; LD = Ludlowville Formation; GS = Geneseo Formation; WR = West River Formation; MX = Middlesex Formation; CA = Cashaqua Formation; RS = Rhinestreet Formation; AN = Angola Formation; PC = Pipe Creek Formation; HA = Hanover Formation; DK = Dunkirk Formation; GO = Gowanda Formation; (B) map displaying concretion sampling locations in western New York State. Refer to Table 1 for details of individual concretions, including sample locations.

Borowski et al., 1999; Boetius et al., 2000; Paull et al., 2000). Low sedimentation rates focus the diagenetic effects of AOM, maintaining elevated pore water alkalinity within the SMTZ for an extended period of time (Borowski et al., 1999; Rodriguez et al., 2000; D'Hondt et al., 2004; Snyder et al., 2007; Dickens and Snyder, 2009). The formation of the studied carbonate concretions as a consequence of AOM is buttressed by their association with ^{34}S-enriched pyrite and barite (Lash, 2015a,b), an argument made by Borowski et al. (2013) based on their investigation of younger methane-bearing marine deposits of the Blake Ridge.

4.1. Timing of concretion growth

Canfield and Raiswell (1991) argue convincingly that the timing of concretion growth is best deduced by assessing the degree of compaction of encapsulating shale at the time of concretion formation. The wrapping of Devonian concretions by laminated shale (Fig. 2B,E) is consistent with their formation at shallow burial depths early in the compaction history of these deposits (Lash and Blood, 2004b). Further, SEM analysis of host shale samples collected from adjacent to lateral edges of concretions reveals a modestly open clay grain microfabric (Lash and Blood, 2004b). Shale samples collected centimeters away from these areas, however, display a strongly oriented platy grain microfabric (Lash and Blood, 2004b). The former deposits are interpreted to have occupied pressure shadow regions of host sediment that were shielded by adjacent rigid carbonate during early and shallow mechanical compaction (Lash and Blood, 2004b).

A shallow depth of concretion formation is further suggested by the pervasive occurrence of randomly oriented clay grains reminiscent of clay floccules within concretions (e.g., O'Brien, 1981; O'Brien and Slatt, 1990; Bennett et al., 1991; Slatt and O'Brien, 2013) (Fig. 3A). The depositional texture of the host clay was likely shielded from compaction-related grain reorientation by the precipitation of calcium carbonate soon after deposition. Similarly, algal cysts ranging from 60 to 120 μm

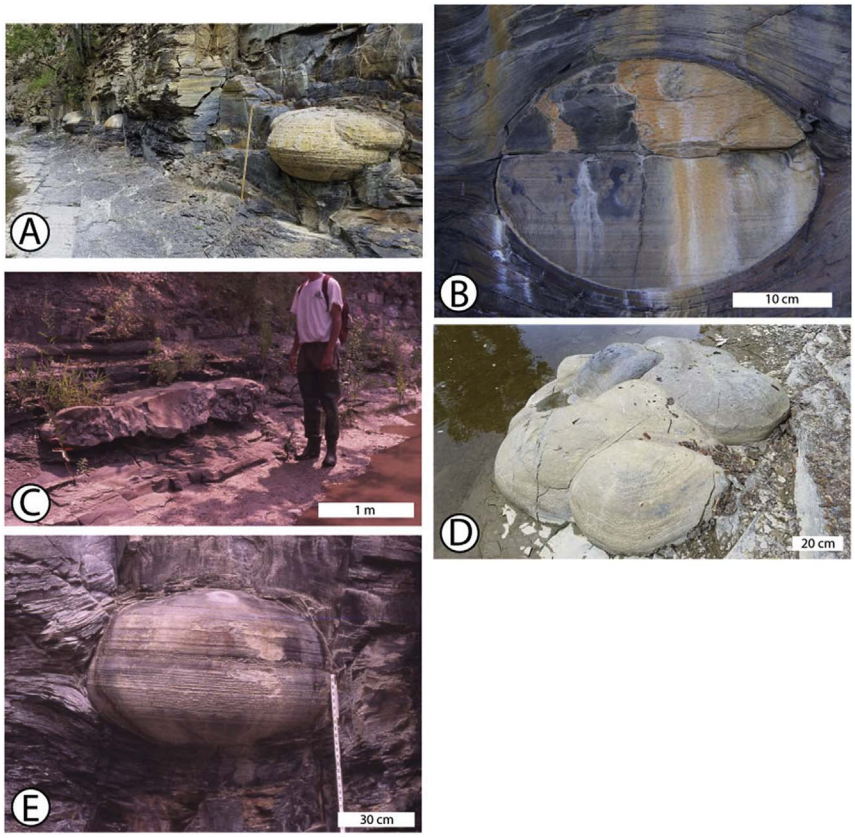

Fig. 2. Field photographs of carbonate concretions displaying textural aspects described in the text. Concretion RSTA is the only isotopically analyzed concretion included in the group of field images; (A) carbonate concretion horizon in the lower Rhinestreet Formation; measuring stick = 1 m (42.700° N; 78.898° W); (B) carbonate concretion (RSTA) of the Rhinestreet Formation displaying internal laminae; note wrapping of host shale around the concretion (42.699° N; 79.897° W); (C) elongate carbonate concretion hosted by organic-deficient gray shale in the upper Rhinestreet Formation (42.688° N; 78.877° W); (D) coalesced carbonate concretion in the lower Dunkirk Formation (42.510° N; 79.172° W); (E) laminated carbonate concretion in the lower Rhinestreet Formation (42.699° N; 78.897° W).

Table 1
Concretion data[1].

Concretion identifier	Host unit	Latitude	Longitude	Diameter (cm)	Center $\delta^{13}C$ ‰ V-PDB	Edge $\delta^{13}C$ ‰ V-PDB
KC	Gowanda	42.496°N	79.164°W	14	-1.43	-0.21
GOL	"	42.499°N	79.166°W	23	-8.87	-2.45
DK	Dunkirk	42.507°N	79.174°W	124	-12.01	-0.15
LDK	"	42.510°N	79.172°W	19.5	-10.03	-0.85
HAC[2]	**Hanover**	**42.534°N**	**79.168°W**	**19**	**-5.04**	**-6.03**
HAC2	"	42.522°N	79.165°W	31	-8.43	-0.67
ANG	Angola	42.670°N	79.861°W	35.9	-16.9	-7.49
SPGSC	Rhinestreet	42.692°N	78.042°W	118	-13.46	-4.52
RST1	"	42.699°N	79.897°W	19.5	-4.97	0.27
RSTA	**"**	**"**	**"**	**34**	**4.01**	**-4.99**
UC	"	"	"	72	-11.73	2.26
LC1	"	42.688°N	79.878°W	125	-13.05	-0.81
RSC	"	"	"	54	-12.03	-0.45
SPC	"	42.687°N	78.876°W	98	-5.07	2.53
C1	"	42.691°N	78.931°W	118	-12.01	-0.75
C2[3]	"	"	"	130	-12.05	-0.54; -6.06
EMC29	"	"	"	52	-15.12	-1.75
LCC	Cashaqua	42.701°N	78.948°W	34	-7.85	-0.35
CAC	"	42.696°N	78.935°W	23	-8.01	-12.55
CC4	**"**	**42.700°N**	**78.943°W**	**18**	**-8.51**	**-12.46**
GEN1	Geneseo	42.900°N	78.423°W	29	-10.02	-6.02
LUD	Ludlowville	42.710°N	78.980°W	24	-8.72	-5.98
Mar1	**Marcellus**	**42.978°N**	**77.989°W**	**37**	**-12.34**	**-15.01**
Mar2	"	42.980°N	77.989°W	17	-13.54	-10.62

[1]Gray shading denotes those concretions collected from organic-deficient gray shale.
[2]Bold lettering designates those concretions displaying center-to-edge profiles of decreasing $\delta^{13}C$.
[3]Concretion C2 displays a center-to-edge isotope profile of increasing $\delta^{13}C$ to a value of -0.54‰ approximately 12 cm from the edge of the concretion beyond which $\delta^{13}C$ diminishes to -6.06‰ at the margin (Fig. 5).

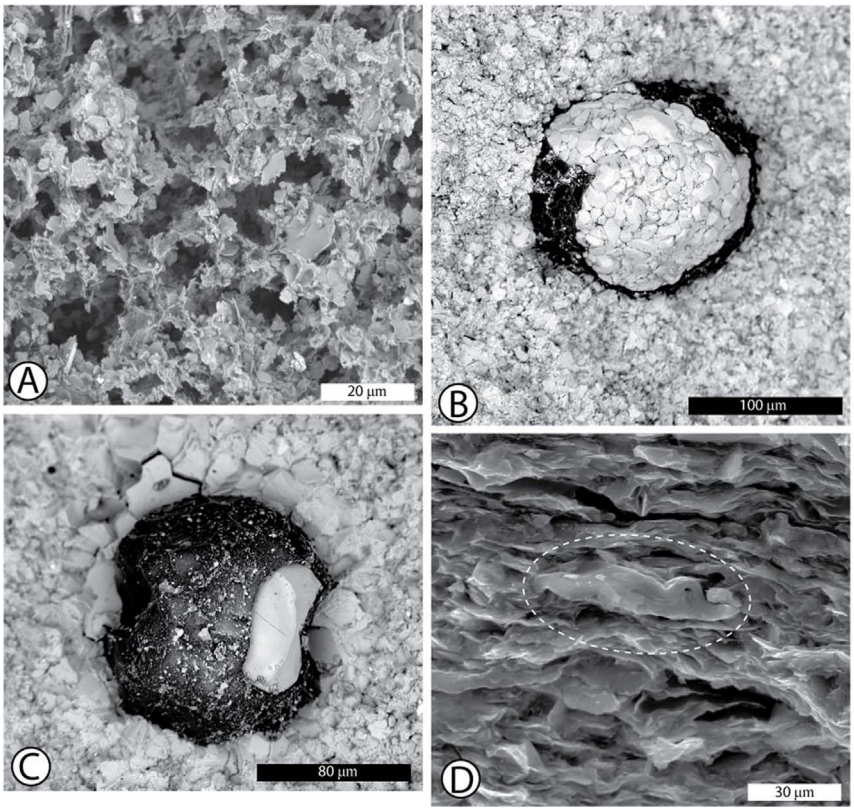

Fig. 3. SEM images of micro-textural features of Middle and Upper Devonian concretions; (A) etched concretion sample from the edge of concretion UC, Rhinestreet Formation; (B, C) spherical algal cysts in samples from the edge (B) and center (C) of concretion Mar1, Marcellus Formation; (D) host shale displaying a strongly oriented clay grain microfabic and a flattened algal cyst (indicated by dashed white oval) from a sample collected adjacent to concretion C2, Rhinestreet Formation.

in diameter observed in samples collected from throughout concretions display their original spherical shapes (Fig. 3B and C). The spherical structures, like the depositional clay grain microfabric, appear to have been protected from burial-related flattening (Fig. 3D) by the pervasive precipitation of microcrystalline calcite cement.

The duration of formation of the studied concretions cannot be quantified, yet micro-textural features suggest that they precipitated rapidly at shallow depth, perhaps several meters to a few tens of meters below the sediment-water interface (SWI) (Lash and Blood, 2004a,b). The uniformly very-fine grain size (15–25 μm) of matrix carbonate and lack of textural evidence of growth banding evince a rapid growth history of a single generation of calcite microspar (Selles-Martinez, 1996; Mozley, 1996; Raiswell and Fisher, 2000, 2004; Gaines and Vorhies, 2016).

4.2. Mode of concretion growth

Concretions hosted by black shale display depositional laminae inherited from the host sediment that accumulated under oxygen-depleted conditions thereby limiting or precluding the activity of bioturbating organisms (Fig. 2B,E) (Lash and Blood, 2004a). It is noteworthy that laminae do not thin systematically from concretion centers to edges as would be expected of carbonate masses that precipitated radially coincident with burial-related compaction. Rather, it appears that the concretion masses formed at an essentially steady depth below the SWI. Indeed, the omnipresence of spherical algal cysts and clay floccules within concretions is suggestive of a generally pervasive growth history that entailed the infilling of void space in the host sediment. It is noteworthy, though, that the studied concretions display constant or modestly diminishing carbonate (reflected in Ca abundances) from concretion centers to edges (Fig. 4A) (Lash and Blood, 2004a), perhaps an indicator of outward decreasing porosity of the host sediment at some point in their formation history (e.g., Raiswell, 1976; Coleman and Raiswell, 1981). However, the fact that the infilling of pore space by calcite cement may be attended by some degree of grain displacement (e.g., Raiswell and Fisher, 2000; Bojanowski and Clarkson, 2012) cautions against inferring a simple relationship between the abundance of carbonate cement and sediment porosity. Indeed, Lash and Blood (2004a) argued that the passive infilling of pore space within host sediment associated with the formation of concretions of the Rhinestreet Formation was accompanied by some displacement of siliciclastic grains.

4.3. Diagenetic environment of concretion formation - anaerobic oxidation of methane (AOM)

The prevailing view of calcium carbonate precipitation driven by AOM holds that the $\delta^{13}C$ of pore water and authigenic carbonate should reflect the isotopic composition of the methane substrate (i.e., less than −30‰ V-PDB; Borowski et al., 1997; Aloisi et al., 2000). However, recent investigations of pore fluid geochemistry of methane-charged sediments have revealed relatively high $\delta^{13}C_{DIC}$ values (> - 20‰ V-PDB) within SMTZs reflecting the commingling of DIC generated by organic matter degradation and methanogenesis at depth with that produced *in situ* by AOM at the SMTZ (Rodriguez et al., 2000; Borowski et al., 2000; Sivan et al., 2007; Snyder et al., 2007; Kastner et al., 2008; Dickens and Snyder, 2009; Chatterjee et al., 2011; Kim et al., 2011; Malinverno and Pohlman, 2011).

The modestly ^{13}C-enriched stable carbon isotope values documented from concretions throughout the Devonian shale succession of the Appalachian Basin by previous studies (Dix and Mullins, 1987; Siegel et al., 1987; Criss et al., 1988; Coniglio and Cameron, 1990; Lash and Blood, 2004a; Lash, 2015a,b) could reflect abnormally high DIC contributions from organoclastic sulfate reduction (OSR) in the bacterial sulfate reduction zone (BSRZ) (Nyman and Nelson, 2011; Teichert et al., 2014). Indeed, Raiswell and Fisher (2004) posited that large calcium carbonate concretions described from outcrop may originate in the BSRZ. They add, though, that calcium carbonate precipitated in this diagenetic zone is limited to no more than porous, low-density masses of approximately 1.5 wt % calcite rigid enough to preserve the

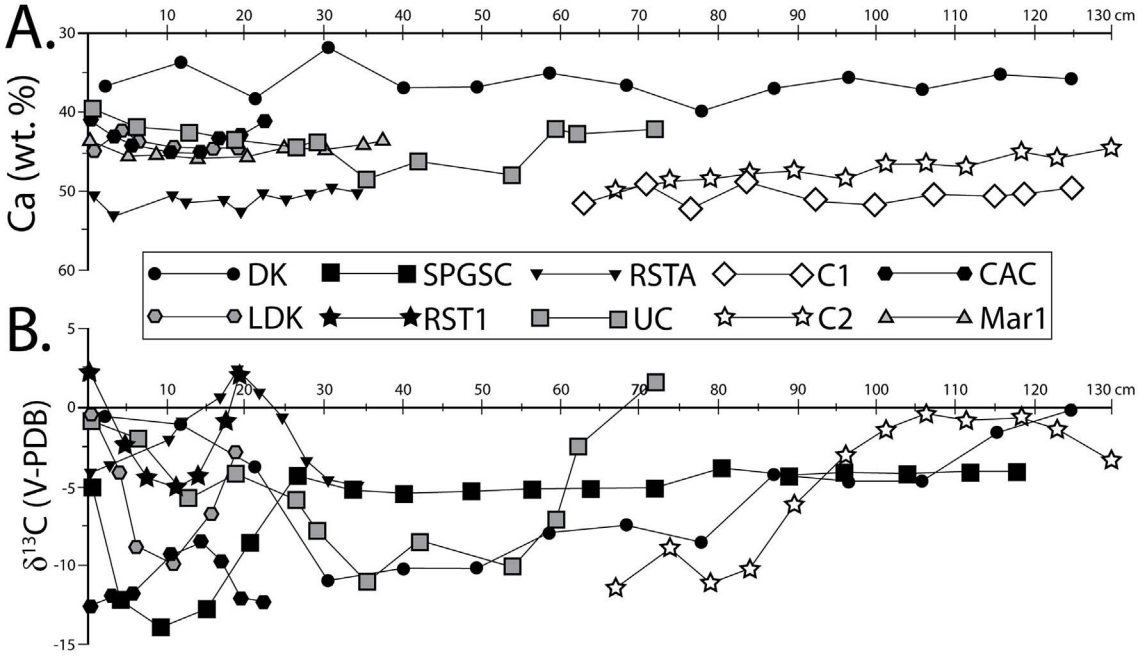

Fig. 4. Edge-to-edge and center-to-edge (open symbols; concretions C1 and C2) profiles of (A) calcium concentration and (B) $\delta^{13}C$ of selected carbonate concretions.

depositional clay grain microfabric of the host sediment. Raiswell and Fisher (2004) further suggest that the dense bodies of concretionary cement observed in outcrop likely record the diagenetic imprint of the faster rates of sulfate reduction and consequent elevated alkalinities generated in association with AOM focused at the SMTZ by diminished sedimentation rates. Thus, the Middle and Upper Devonian concretion horizons are interpreted to reflect growth histories that were initiated within the BSRZ. However, it was not until the nascent concretions were buried to the SMTZ, perhaps a few tens of meters below the SWI (e.g., Borowski et al., 2013), that the dense carbonate masses observed in field exposure formed as a consequence of the passive infilling of porosity. Thus, the discrete calcium carbonate-bearing stratigraphic horizons hosted by the Middle and Upper Devonian shale succession of the western New York region of the Appalachian Basin preserve the record of paleo-SMTZs, each one associated with an episode of reduced sedimentation rate.

The widespread distribution of carbonate concretions throughout the Devonian shale succession of the Appalachian Basin (Siegel et al., 1987; Dix and Mullins, 1987; Criss et al., 1988; Coniglio and Cameron, 1990; Enomoto et al., 2012) suggests that methane transport was diffusion-dominant, perhaps enhanced by burial-induced advection (e.g., Ritger et al., 1987). There is no evidence that methane advected rapidly along faults and/or inclined permeable layers, or that methane was transported directly to the SWI as cold seeps. Further, geological considerations provide no evidence that methane was sourced in underlying methane hydrate systems (Lash, 2015a). It is likely, then, that most or all methane ascending the Devonian sedimentary column was consumed by AOM at numerous SMTZs, each one stabilized during a period of reduced sedimentation rate. Indeed, the diffusional nature of methane transport in the Appalachian Basin may account for isotopic differences between the studied Devonian concretions and authigenic carbonate described from many recent and modern methane-charged sedimentary systems. That is, most discussions focusing on authigenic carbonate precipitation in association with AOM address marine sediments overlying methane hydrate systems that typically yield higher methane fluxes and, therefore, higher rates of AOM (Smith and Coffin, 2014).

5. Stable carbon isotope profiles

The majority (75%) of the 24 analyzed concretions display radial profiles of increasing bulk $\delta^{13}C$ (Fig. 4B; Table 1), similar to observations elsewhere in the Appalachian Basin (Dix and Mullins, 1987; Siegel et al., 1987; Criss et al., 1988; Coniglio and Cameron, 1990). Center-to-edge $\delta^{13}C$ variations range from 1.41‰ to 13.37‰ with most values exceeding 9‰ (Table 1). Minimum $\delta^{13}C$ values near concretion centers range from −15.12‰ to −1.43‰ whereas edge values range from −10.62‰ to 2.53‰ (Table 1). It is noteworthy that smaller concretions (i.e., less than ~ 50 cm in diameter) tend to display the least amount of radial $\delta^{13}C$ variation (Table 1). Though isotope profiles are generally symmetrical, their lowest values near the geometric centers of concretions, concretion SPGSC in the lower part of the Rhinestreet Formation (Fig. 1A) displays rapid increases of $\delta^{13}C$ in both directions from a minimum $\delta^{13}C$ value approximately 12 cm from the concretion margin (Fig. 4B).

Four concretions analyzed as part of the present study exhibit center-to-edge profiles of diminishing $\delta^{13}C$ (Table 1), a trend that has been reported from some Devonian concretions elsewhere in the basin (Dix and Mullins, 1987). Concretions featuring this type of profile occur throughout the studied succession, including the Rhinestreet, Marcellus, and Cashaqua formations (Table 1). It is noteworthy that Rhinestreet concretion RSTA, displaying a profile of decreasing $\delta^{13}C$, was collected within the same stratigraphic interval as concretions UC and RST1, both of which display the more common radial profile of increasing $\delta^{13}C$ (Fig. 4B; Table 1). The center $\delta^{13}C$ value of concretion RSTA (4.01‰) diminishes 9‰ outward (Fig. 4B; Table 1) to a value of –4.99‰, approximately equal to the edge $\delta^{13}C$ value of nearby concretion RST1, - 4.97‰ (Table 1). Two concretions display center-to-edge variation of less than 1.5‰ (Table 1). These concretions, one each from the Gowanda (KC) and Hanover (HAC) formations, are small, 13 cm and 18 cm in diameter, respectively (Table 1). The former displays $\delta^{13}C$ values that concentrate close to 0‰, whereas concretion HAC displays little variation about a $\delta^{13}C$ value of approximately −5.5‰ (Table 1). In detail, however, concretion KC displays a slight radial $\delta^{13}C$ increase whereas concretion HAC appears to record a minor center-to-edge trend of diminishing $\delta^{13}C$ (Table 1).

Perhaps the most intriguing $\delta^{13}C$ trend is displayed by concretion

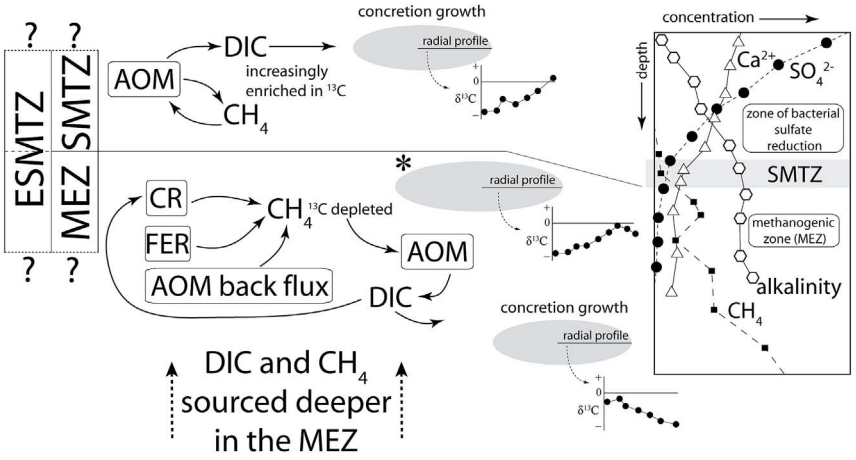

Fig. 5. Cartoon illustrating the range of processes that may contribute to the isotopic composition of DIC within and close to the SMTZ. Depth – concentration profiles of aqueous Ca^{2+}, SO_4^{2-}, alkalinity, and CH_4 are hypothetical and based on Raiswell and Fisher (2004) and Snyder et al. (2007). The base of the SMTZ on the depth – concentration profile is traced to the left part of the figure. Columns on the far left depict the methanogenic zone (MEZ) and overlying sulfate-methane transition zone (SMTZ) where anaerobic oxidation of methane (AOM) may occur under methane-limited conditions yielding the common center-to-edge profiles of increasing $\delta^{13}C$. The extended sulfate-methane transition zone (ESMTZ; Hong et al., 2013) includes the sulfate-depleted upper MEZ where strongly ^{13}C-depleted methane may be produced by carbon dioxide reduction (CR), organic matter degradation by fermentation (FER), and AOM back flux thereby fueling AOM and favoring the development of radial isotope profiles of decreasing $\delta^{13}C$. Fluctuations of methane delivery from deeper sources will cause the boundary between the SMTZ and MEZ to shift resulting in changing diagenetic conditions within the ESMTZ. For example, increasing methane flux may be recorded by the center-to-edge trend of increasing followed by decreasing $\delta^{13}C$ (e.g., concretion C2). Modified from Hong et al. (2013) and Yoshinaga et al. (2014).

C2 hosted by the Rhinestreet Formation (Fig. 4B). This concretion, approximately 1.3 m wide, displays a radial profile of increasing $\delta^{13}C$ over much of its volume. However, the outer approximately 12 cm of the carbonate mass exhibits a $\delta^{13}C$ reduction of approximately 6‰ (Fig. 4B).

6. Discussion

The precipitation of authigenic calcium carbonate is not accompanied by fractionation of stable carbon isotopes (Teichert et al., 2005). Thus, isotope profiles displayed by concretions record compositional changes of DIC contemporaneous with carbonate precipitation. Radial profiles of increasing $\delta^{13}C$ have been attributed to the progressive ^{13}C enrichment of DIC as the host sediment was buried from the BSRZ into the MEZ (Raiswell, 1971; Curtis et al., 1986; Dix and Mullins, 1987; Astin and Scotchman, 1988; Coniglio and Cameron, 1990; Scotchman, 1991; Jordan et al., 1992). However, this interpretation is not compatible with textural evidence suggesting that the bulk of the analyzed Middle and Upper Devonian concretions precipitated at essentially constant burial depth, within the SMTZ. More importantly, it fails to account for those concretions displaying center-to-edge profiles of decreasing $\delta^{13}C$. Raiswell (1987) attributed radial profiles of increasing $\delta^{13}C$ documented from concretions inferred to have formed in association with AOM to the progressive ^{13}C-enrichment of DIC diffusing upward from the MEZ to the SMTZ. This explanation does not offer a satisfactory solution for the repeated occurrences of concretions displaying center-to-edge profiles of increasing $\delta^{13}C$ from the Middle Devonian Marcellus Formation into the Upper Devonian Gowanda Formation (Fig. 1A; Table 1). That is, the long-term isotopic evolution of methane produced in the MEZ would be revealed by increasing ^{13}C-enrichment of $\delta^{13}C$ values up-section, which is not evident in the studied Middle and Upper Devonian succession.

In general, explanations of radial $\delta^{13}C$ profiles displayed by carbonate concretions formed in association with AOM rely on processes external to the SMTZ, principally the methanogenic production of ^{13}C-enriched DIC. Little discussion has focused on AOM as a mechanism of isotope fractionation within and near the SMTZ. It is widely recognized that bacterially mediated reactions associated with AOM discriminate against the heavier carbon isotope (Yoshinaga et al., 2014). Over time and with limited methane delivery to the SMTZ, however, AOM leaves the residual methane pool of the SMTZ enriched in heavier carbon (Barker and Fritz, 1981; Alperin and Reeburgh, 1985; Whiticar and Faber, 1986; Alperin et al., 1988; Holler et al., 2009). Bicarbonate produced by AOM, though more enriched in ^{12}C than residual methane, follows a trend of increasing $\delta^{13}C$ over time. The common center-to-edge profiles of increasing $\delta^{13}C$ of the studied Middle and Upper Devonian concretions likely reflect ^{13}C enrichment of DIC coeval with concretion formation under methane-limited conditions. Thus, each pause in sedimentation during accumulation of the Devonian shale succession was accompanied by the focusing of AOM-related carbon fractionation at each paleo-SMTZ. It is noteworthy that the typical radial isotope variation displayed by the studied Devonian concretions of less than 10‰ is consistent with what is known of AOM-related isotope fractionation (Sivan et al., 2007). Carbon isotope fractionation associated with AOM under methane-limited conditions, while offering an explanation for the common radial profiles of increasing $\delta^{13}C$, fails to account for the few concretions displaying center-to-edge trends of diminishing $\delta^{13}C$. Indeed, any interpretation of the isotopic evolution of these concretions must be consistent with their formation in association with AOM and essentially contemporaneous with concretions displaying the more common profiles of increasing $\delta^{13}C$.

Recent studies have revealed the presence of low concentrations of strongly ^{13}C-depleted methane within and immediately below some SMTZs (Borowski et al., 1997; Paull et al., 2000; Hoehler et al., 2000; Pohlman et al., 2008; Colwell et al., 2008; Hong et al., 2013, 2014; Geprägs et al., 2016). Production of this methane has been attributed to the reduction of carbon dioxide (bicarbonate) generated by AOM (Borowski et al., 1997) and/or the production of hydrogen via the formation of pyrite from sulfide formed in association with AOM (Hong et al., 2013, 2014). In addition to carbon dioxide reduction (CR), fermentation (FER) within sediment immediately below the SMTZ is known to produce ^{13}C-depleted methane (Claypool et al., 2006; Colwell et al., 2008; Hong et al., 2013, 2014). The presence of ^{13}C-depleted methane within SMTZs has also been ascribed to AOM back flux, a reverse isotope effect related to the enzyme-level reversibility of AOM under sulfate-limited diagenetic conditions (Yoshinaga et al., 2014; Geprägs et al., 2016; Egger et al., 2016). The production of methane within and near the SMTZ by any or all of the mentioned mechanisms fuels AOM and helps to stabilize the SMTZ when methane flux is low (Hong et al., 2014).

The described diagenetic environment established at each SMTZ in association with AOM would have left an isotopic imprint on DIC perhaps more varied than that reflective of the isotopic composition of methane and DIC originating within the MEZ (Hong et al., 2014) (Fig. 5). Indeed, the contrasting radial stable carbon isotope profiles of the Middle and Upper Devonian concretions likely reflects the complicated nature of carbon cycling close to and within SMTZs (e.g., Holler et al., 2009; Malinverno and Pohlman, 2011; Hong et al., 2013, 2014; Yoshinaga et al., 2014; Geprägs et al., 2016; Timmers et al., 2017). Most of the studied Middle and Upper Devonian concretions appear to have formed in association with AOM under what was likely methane-limited diagenetic conditions (Yoshinaga et al., 2014) that

favored the enrichment of residual methane and produced carbon dioxide (bicarbonate) in heavy carbon (Barker and Fritz, 1981). On the other hand, anaerobic oxidation of ^{13}C-depleted methane generated by CR or AOM back flux may be recorded by the scarce concretions displaying center-to-edge gradients of decreasing $\delta^{13}C$. The close association of concretions exhibiting contrasting $\delta^{13}C$ profiles within the same stratigraphic interval (e.g., concretions RSTA, UC, and RST1, Table 1) suggests that paleo-SMTZs within the Middle and Upper Devonian shale succession experienced fluctuations in methane and/or sulfate fluxes that would have favored the occurrence, at least temporarily, of CR and/or AOM back flux and related production of ^{13}C-depleted methane. Indeed, both processes appear to be associated with sulfate-limited diagenetic conditions that would be expected of the lower SMTZ and immediately underlying upper MEZ (Hong et al., 2013; Yoshinaga et al., 2014) (Fig. 5).

Hong et al. (2013, Fig. 1), cognizant of the interrelated nature of processes associated with carbon cycling within and near the SMTZ, included an interval of ^{13}C-depleted methanogenesis in the lower part of an expanded SMTZ (ESMTZ; Fig. 5). Similarly, Yoshinaga et al. (2014, Fig. 3) extended the diagenetic zone in which AOM occurs into the upper MEZ where ^{13}C-depleted methane may be produced by AOM back flux (Fig. 5). Fluctuating methane delivery could have induced small (a few tens of cm) vertical movements of the boundary separating the upper and lower ESMTZ (Fig. 5) thereby causing the diagenetic environment to change from that favoring AOM to one dominated by AOM back flux and/or CR. Indeed, the rare concretions displaying minimal center-to-edge variation of $\delta^{13}C$ may record carbonate precipitation histories during which the internal boundary of the ESMTZ remained stationary resulting in little more than a muted radial $\delta^{13}C$ profile of increasing (concretion KC) or decreasing (concretion HAC) $\delta^{13}C$ (Fig. 5).

Hong et al. (2014) maintain that variable methane flux can cause changes in the relative significance of AOM and CR. Specifically, increasing methane delivery and consequent shoaling of the boundary separating the upper and lower ESMTZ may induce a shift from AOM to AOM back flux or CR (Fig. 5; Yoshinaga et al., 2014; Hong et al., 2014). An example of such a change in diagenetic environment may be preserved in the isotope profile of concretion C2 of the Rhinestreet Formation (Fig. 4B) in which increasing $\delta^{13}C$ outward from the concretion center diminishes through the outer 12 cm of the concretion (Fig. 5).

The scarcity of studied carbonate concretions displaying radial profiles of decreasing $\delta^{13}C$ may reflect (1) a higher rate of aqueous Ca^{2+} removal associated with methane-limited concretion growth higher in the ESMTZ (e.g., Raiswell and Fisher, 2004) and/or (2) a limited amount of more strongly ^{13}C-depleted methane produced in association with AOM back flux and/or CR (Geprägs et al., 2016) (Fig. 5). It is noteworthy, however, that the sulfate-deficient nature of the diagenetic environment postulated to have favored the production of ^{13}C-depleted methane was not an impediment to AOM. It is increasingly apparent that AOM can proceed at sulfate concentrations of 0.5 nM or less (Treude et al., 2005; Knab et al., 2009; Beal et al., 2011).

7. Conclusions

Carbonate concretions are ubiquitous throughout the Middle and Upper Devonian shale succession of western New York State. They are typically concentrated within discrete 1- to 2-m-thick stratigraphic horizons hosted by carbonaceous black shale and organic-deficient gray shale. Textural characteristics of concretions, including an open detrital clay grain microfabric typical of newly deposited clay floccules as well as spherical algal cysts preserved throughout concretion bodies and laminae that maintain constant center-to-edge thickness, are consistent with their formation in the BSRZ as low-density, compaction-resistant calcium carbonate masses. Subsequent burial of the incipient concretions to the SMTZ, stabilized during periods of reduced sedimentation rate, was accompanied by the nearly complete infilling of porosity in association with AOM.

The generally ^{13}C-enriched nature of Appalachian Basin concretionary carbonate may reflect the commingling of fluids external to the SMTZ, including methane, methanogenic biocarbonate, and perhaps pore fluid originating from underlying carbonate units (Onondaga Limestone; Lindemann, 1995), ascending the sediment column. However, dissimilar radial $\delta^{13}C$ profiles of the studied concretions likely reflect the complex nature of carbon cycling associated with AOM close to and within the SMTZ rather than variations in the isotopic composition of DIC originating in deeper sources. The common center-to-edge profile of increasing $\delta^{13}C$ documented from concretions throughout the studied shale succession may be attributed to AOM-related kinetic isotopic fractionation and consequent increasing $\delta^{13}C$ of residual methane and produced DIC. Such a diagenetic history is favored by methane-limited diagenetic conditions. Markedly fewer concretions displaying radial profiles of decreasing $\delta^{13}C$ may reflect the diagenetic signature of secondary methanogenesis (CR, FER) and/or AOM back flux. Anaerobic oxidation of strongly ^{13}C-depleted methane produced by these processes, which appear to be favored under sulfate-limited conditions more typical of the lower SMTZ and upper MEZ, may have induced a shift of $\delta^{13}C_{DIC}$ to lighter values during AOM-related carbonate precipitation. The postulated scenario is consistent with the concept of an expanded SMTZ comprised of an upper methane-depleted horizon and an underlying sulfate-deficient interval that includes the upper MEZ. Subtle variations of methane flux could have induced small vertical shifts of the boundary of separating the two diagenetic zones resulting in the juxtaposition of texturally similar concretions reflecting different diagenetic histories.

Acknowledgments

Much appreciation is due Walter Borowski and the anonymous reviewer for their efforts to improve the manuscript. ThermoFisher, Chesapeake Energy Corporation, and Vista Resources are thanked for their financial support of this work. Steve Saboda and Randy Blood are acknowledged for their assistance in the field over the years.

References

Aloisi, G., Pierre, C., Rouchy, J.M., Foucher, J.P., Woodside, J., 2000. Methane-related authigenic carbonates of eastern Mediterranean Sea mud volcanoes and their possible relation to gas hydrate destabilization. Earth Planet Sci. Lett. 184, 321–338.

Alperin, M.J., Reeburgh, W.S., 1985. Inhibition experiments on anaerobic methane oxidation. Appl. Environ. Microbiol. 50, 940–945.

Alperin, M.J., Reeburgh, W.S., Whiticar, M.J., 1988. Carbon and hydrogen isotope fractionation resulting from anaerobic methane oxidation. Global Biogeochem. Cycles 2, 279–288.

Astin, T.R., Scotchman, I.C., 1988. The diagenetic history of some septarian concretions from the Kimmeridge Clay, England. Sedimentology 35, 349–368.

Baird, G.C., Lash, G.G., 1990. Devonian Strata and Environments: Chautauqua County Region: New York State Geological Association, 62nd Annual Meeting Guidebook, Sat. pp. A1–A46.

Barker, J.F., Fritz, P., 1981. Carbon isotope fractionation during microbial methane oxidation. Nature 293, 289–291.

Beal, E.J., Claire, M.W., House, C.H., 2011. High rates of anaerobic methanotrophy at low sulfate concentrations with implications for past and present methane levels. Geobiology 9, 131–139.

Bennett, R.H., O'Brien, N.R., Hulbert, M.H., 1991. Determinants of clay and shale microfabric signatures: processes and mechanisms. In: Bennett, R.H., Bryant, W.R., Hulbert, M.H. (Eds.), Microstructure of Fine-grained Sediments. Springer-Verlag, New York, pp. 5–31.

Boetius, A., Ravenschlag, K., Schubert, C.J., Rickert, D., Widdel, F., Gieseke, A., Amann, R., Jørgensen, B.B., Witte, U., Pfannkuche, O., 2000. A marine microbial consortium apparently mediating anaerobic oxidation of methane. Nature 407, 623–626.

Bojanowski, M.J., Clarkson, E.N.K., 2012. Origin of siderite concretions in microenvironments of methanogenesis developed in a sulfate reduction zone: an example or a rule? J. Sediment. Res. 82, 585–598.

Borowski, W.S., Paull, C.K., Ussler III, W., 1997. Carbon cycling within the upper Methanogenic zone of continental-rise sediments: an example from the methane-rich Sediments overlying the Blake Ridge gas hydrate deposits. Mar. Chem. 57, 299–311.

Borowski, W.S., Paull, C.K., Ussler III, W., 1999. Global and local variations of interstitial sulfate gradients in deep-water, continental margin sediments: sensitivity to underlying methane and gas hydrates. Mar. Geol. 159, 131–154.

Borowski, W.S., Hoehler, T.M., Alperin, M.J., Rodriguez, N.M., Paull, C.K., 2000.

Significance of anaerobic methane oxidation in methane-rich sediments overlying the Blake Ridge gas hydrate. In: In: Paull, C.K., Matsumoto, R., Wallace, P.J., Dillon, W.P. (Eds.), Proceedings of the Ocean Drilling Program, Scientific Results, vol. 164. pp. 87–99.
Borowski, W.S., Rodriguez, N.M., Paull, C.K., Ussler III, W., 2013. Are ^{34}S-enriched authigenic sulfide minerals a proxy for elevated methane flux and gas hydrates in the geologic record? Mar. Petrol. Geol. 43, 381–395.
Canfield, D.E., Raiswell, R., 1991. Carbonate precipitation and dissolution. In: Allison, P.S.A., Briggs, D.E.G. (Eds.), Taphonomy: Releasing the Data Locked in the Fossil Record. Plenum Press, New York, pp. 411–453.
Chatterjee, S., Dickens, G.R., Bhatnager, G., Chapman, W.G., Dugan, B., Snyder, G.T., Hiraski, G.J., 2011. Pore water sulfate, alkalinity, and carbon isotope profiles in shallow sediment above marine gas hydrate systems: a numerical modeling perspective. J. Geophys. Res. 116, B09103. http://dx.doi.org/10.1029/2011JB008290.
Claypool, G.E., Milikov, A.V., Lee, Y.-J., Torres, M.E., Borowski, W.S., Tamaru, H., 2006. Microbial methane generation and gas transport in shallow sediments of an accretionary complex, Southern Hydrate Ridge (ODP Leg 204), offshore Oregon, USA. In: In: Trehu, A.M., Bohrmann, G., Torres, M.E., Colwell, F.S. (Eds.), Proceedings of the Ocean Drilling Program, Scientific Results, vol. 204. pp. 1–52.
Coleman, M.L., Raiswell, R., 1981. Carbon, oxygen and sulphur isotope variation in carbonate concretions from the Upper Lias of NE England. Geochem. Cosmochim. Acta 45, 329–340.
Colwell, F.S., Boyd, S., Delwicbe, M.E., Reed, D.W., Phelps, T.J., Newby, D.T., 2008. Estimates of biogenic methane production rates in deep marine sediments at Hydrate Ridge. Cascadia Margin. Appl. Environ. Microbiol. 74, 3444–3457.
Coniglio, M., Cameron, J.S., 1990. Early diagenesis in a potential oil shale: evidence from calcite concretions in the Upper Devonian Kettle Point Formation, southwestern Ontario. Bull. Can. Petrol. Geol. 38, 64–77.
Criss, R.E., Cooke, G.A., Day, S.D., 1988. An organic origin for the carbonate concretions of the Ohio Shale. U. S. Geol. Surv. Bull. 1836 21 p.
Curtis, C.D., Petrowski, C., Oertel, G., 1972. Stable carbon isotope ratios within carbonate concretions: a clue to place and time of formation. Nature 235, 98–100.
Curtis, C.D., Coleman, M.L., Love, L.G., 1986. Pore water evolution during sediment burial from isotopic and mineral chemistry of calcite, dolomite and siderite concretions. Geochim. Cosmochim. Acta 50, 2321–2334.
D'Hondt, S.L., Jørgensen, B.B., Miller, D.J., et al., 2004. Distributions of microbial activities in deep subseafloor sediments. Science 306, 2216–2221.
Day-Stirrat, R.J., Loucks, R.G., Milliken, K.L., Hillier, S., van der Pluijm, B.A., 2008. Phyllosilicate orientation demonstrates early timing of compactional stabilization in calcite-cemented concretions in the Barnett Shale (Late Mississippian), Fort Worth Basin, Texas (USA). Sed. Geol. 208, 27–35.
Dickens, J., Snyder, G.T., 2009. Interpreting upward methane flux from pore water profiles. Fire in the ice, national energy technology laboratory methane hydrate newsletter. Winner 7–10.
Dix, G.R., Mullins, H.T., 1987. Shallow, subsurface growth and burial alteration of Middle Devonian calcitic concretions. J. Sediment. Petrol. 57, 140–152.
Egger, M., Kraal, P., Jilbert, T., Sulu-Gambari, F., Sapart, C.J., Röckmann, T., Slomp, C.P., 2016. Anaerobic oxidation of methane alters sediment records of sulfur, iron and phosphorus in the Black Sea. Biogeosciences 13, 5333–5355.
Enomoto, C.B., Coleman Jr., J.L., Haynes, J.T., Whitmeyer, S.J., McDowell, R.R., Lewis, J.E., Spear, T.P., Swezey, C.S., 2012. Geology of the Devonian Marcellus Shale – Valley and Ridge Province, Virgina and West Virginia – a Field Trip Guide Book for the American Association of Petroleum Geologists Eastern Section Meeting, September 28-29, 2011. U.S. Geol. Surv. Open-file Report 2012-1194. 48 p.
Friedman, G.M., Johnson, K.G., 1966. The Devonian Catskill deltaic complex of New York, type example of a “tectonic delta complex,”. In: Shirley, M.L., Ragsdale, J.A. (Eds.), Deltas in Their Geologic Framework. Houston Geological Society, pp. 171–188.
Gaines, R.R., Vorhies, J.S., 2016. Growth mechanisms and geochemistry of carbonate concretions from the Cambrian Wheeler Formation (Utah, USA). Sedimentology 63, 662–698.
Gautier, D.L., Claypool, G.E., 1984. Interpretation of methane diagenesis in ancient sediments by analogy with processes in modern diagenetic environments. In: In: McDonald, M.A., Surdam, R.C. (Eds.), Clastic Diagenesis: American Association of Petroleum Geologists, Memoir, vol. 37. pp. 111–123.
Geprägs, P., Torres, M.E., Mau, S., Kasten, S., Römer, M., Bohrmann, G., 2016. Carbon cycling fed by methane seepage at the shallow Cumberland Bay, South Georgia, sub-Antarctic. Geochem. Geophys. Geosyst 17, 1401–1418.
Hinrichs, K., Hayes, J.M., Sylva, S.P., Brewer, P.G., DeLong, F., E.F., 1999. Methane-consuming archaebacteria in marine sediments. Nature 398, 802–805.
Hoehler, T.M., Alperin, M.J., Albert, D.B., Martens, C.S., 1994. Field and laboratory studies of methane oxidation in an anoxic marine sediment: evidence for a methanogen-sulfate reducer consortium. Global Biogeochem. Cycles 8, 451–463.
Hoehler, T.M., Borowski, W.S., Alperin, M.J., Rodriguez, N.M., Paull, C.K., 2000. Model, stable isotope, and radiotracer characterization of anaerobic methane oxidation in gas hydrate-bearing sediments of the Blake Ridge. In: In: Paull, C.K., Matsumoto, R., Wallace, P.J., Dillon, W.P. (Eds.), Proceedings of the Ocean Drilling Program, Scientific Results, vol. 164. pp. 79–85.
Holler, T., Wegener, G., Knittel, K., Boetius, A., Brunner, B., Kuypers, M.M.M., Widdel, F., 2009. Substantial ^{13}C/^{12}C and D/H fractionation during anaerobic oxidation of methane by marine consortia enriched in vitro. Environ. Microbiol. Rep 1, 370–376.
Hong, W.L., Torres, M.E., Kim, J.H., Choi, J., Bahk, J.J., 2013. Carbon cycling within the sulfate-methane-transition-zone in marine sediments from the Ulleung Basin. Biogeochemistry 115, 129–148.
Hong, W.L., Torres, M.E., Kim, J.H., Choi, J., Bahk, J.J., 2014. Towards quantifying the reaction network around the sulfate–methane-transition-zone in the Ulleung Basin, East Sea, with a kinetic modeling approach. Geochem. Cosmochim. Acta 140, 127–141.
Hudson, J.D., 1978. Concretion, isotopes and the diagenetic history of the oxford clay (jurassic) of central england. Sedimentology 25, 339–370.
Hudson, J.D., Friedman, I., 1976. Carbon and oxygen isotopes in concretions: relationship to porewater changes during diagenesis. In: Cadek, J., Paces, T. (Eds.), Proc. Internal. Symposium on Water/Rock Interaction, Czechoslovakia. Geol. Survey, Prague, pp. 331–339.
Irwin, H., Curtis, C.D., Coleman, M.L., 1977. Isotopic evidence for source of diagenetic carbonates formed during burial of organic rich sediments. Nature 29, 209–213.
Jordan, M.M., Aplin, A.C., Curtis, C.D., Coleman, M.L., 1992. Access of pore waters to carbonate precipitation sites during concretion growth. Proc. Int. Symp. Water Rock Interact. 7, 1239–1242.
Kastner, M., Claypool, G.E., Robertson, G., 2008. Geochemical constraints on the origin of the pore fluids and gas hydrate distribution at Atwater Valley and Keathley Canyon, Northern Gulf of Mexico. Mar. Petrol. Geol. 25, 860–872.
Kim, J.-H., Park, M.-H., Chun, J.-H., Lee, J.Y., 2011. Molecular and isotopic signatures in sediments and gas hydrate of the central/southwestern Ulleung Basin: high alkalinity escape fuelled by biogenically sourced methane. Geo Mar. Lett. 31, 37–49.
Knab, N.J., Cragg, B.A., Hornibrook, E.R.C., Holmkvist, L., Pancost, R.D., Borowski, C., et al., 2009. Regulation of anaerobic methane oxidation in sediments of the Black Sea. Biogeosciences 6, 1505–1518.
Lash, G.G., 2015a. Authigenic barite nodules and carbonate concretions in the Upper Devonian shale succession of western New York – a record of variable methane flux burial. Mar. Petrol. Geol. 59, 305–319.
Lash, G.G., 2015b. Pyritization induced by anaerobic oxidation of methane (AOM) – an example from the Upper Devonian shale succession, western New York, USA. Mar. Petrol. Geol. 68, 520–535.
Lash, G.G., Blood, D.R., 2004a. Geochemical and textural evidence for early diagenetic growth of stratigraphically confined carbonate concretions, Upper Devonian Rhinestreet black shale, western New York. Chem. Geol. 206, 407–424.
Lash, G.G., Blood, D.R., 2004b. Depositional clay fabric preserved in early diagenetic carbonate concretion pressure shadows, Upper Devonian (Frasnian) Rhinestreet shale, western New York. J. Sediment. Res. 74, 110–116.
Lash, G.G., Blood, D.R., 2014. Organic matter accumulation, redox, and diagenetic history of the Marcellus Formation, southwestern Pennsylvania, Appalachian Basin. Mar. Petrol. Geol. 57, 244–263.
Lindemann, R.H., 1995. Magnitudes of early diagenetic compaction in the Onondaga Limestone of central and eastern New York. Am. Assoc. Petrol. Geol. Bull. 79, 1416.
Malinverno, A., Pohlman, J.W., 2011. Modeling sulfate reduction in methane hydrate-bearing continental margin sediments: does a sulfate-methane transition require anaerobic oxidation of methane? Geochem. Geophy. Geosy. 12, Q07006. http://dx.doi.org/10.1029/2011GC003501.
Mozley, P.S., 1989. Complex compositional zonation in concretionary siderite: implications for geochemical studies. J. Sed. Res. 59, 815–818.
Mozley, P.S., Burns, S.J., 1993. Oxygen and carbon isotopic composition of marine carbonate concretions: an overview. J. Sediment. Petrol. 63, 73–83.
Mozley, P.S., 1996. The internal structure of carbonate concretions in mudrocks: a critical evaluation of the conventional concentric model of concretion growth. Sediment. Geol. 103, 85–91.
Niewöhner, C., Henson, C., Kasten, S., Zabel, M., Schultz, H.D., 1998. Deep sulfate reduction completely mediated by anaerobic methane oxidation in sediments of the upwelling area off Nambia. Geochem. Cosmochim. Acta 62, 455–464.
Nyman, S.L., Nelson, C.S., 2011. The place of tubular concretions in hydrocarbon cold seep systems: late Miocene Urenui Formation, Taranaki Basin, New Zealand. Am. Assoc. Pet. Geol. 95 1895–1524.
O'Brien, N.R., 1981. SEM study of shale fabric – a review. Scanning Electron. Microsc. 1, 569–575.
O'Brien, N.R., Slatt, R.M., 1990. Argillaceous Rock Atlas. Springer-Verlag, New York.
Paull, C.K., Lorenson, T.D., Borowski, W.S., Ussler, W., Olsen, K., Rodriguez, N.M., 2000. Isotopic composition of CH4, CO2 species, and sedimentary organic matter within samples from the Blake Ridge: gas source implications. In: In: Paull, C., Matsumoto, R., Wallace, P.J., Dillon, W.P. (Eds.), Proc. ODP Sci. Res, vol. 164. pp. 67–78.
Plet, C., Grice, K., Pagès, A., Ruebsam, W., Coolen, M.J.L., Schwark, L., 2016. Microbially-mediated fossil-bearing carbonate concretions and their significance for palaeoenvironmental reconstructions: a multi-proxy organic and inorganic geochemical appraisal. Chem. Geol. 426, 95–108.
Pohlman, J.W., Ruppel, C., Hutchinson, D.R., Downer, R., Coffin, R.B., 2008. Assessing sulfate reduction and methane cycling in a high salinity pore water system in the northern Gulf of Mexico. Mar. Petrol. Geol. 25, 942–951.
Raiswell, R., 1971. The growth of Cambrian and Liassic concretions. Sedimentology 17, 147–171.
Raiswell, R., 1976. The microbiological formation of carbonate concretions in the Upper Lias of NE England. Chem. Geol. 18, 227–244.
Raiswell, R., 1987. Non-steady state microbial diagenesis and the origin of carbonate concretions and nodular limestones. In: In: Marshall, J.D. (Ed.), Diagenesis of Sedimentary Sequences, vol. 36. Geological Society, London, Special Publication, pp. 41–54.
Raiswell, R., 1988. A chemical model for the origin of minor limestone-shale cycles by anaerobic methane oxidation. Geology 16, 641–644.
Raiswell, R., Fisher, Q.J., 2000. Mudrock-hosted carbonate concretions: a review of growth mechanisms and their influence on chemical and isotopic composition. J. Geol. Soc. London 157, 239–251.
Raiswell, R., Fisher, Q., 2004. Rates of carbonate cementation associated with sulphate reduction in DSDP/ODP sediments: implications for the formation of concretions. Chem. Geol. 211, 71–85.

Reeburgh, W.S., 1976. Methane consumption in Cariaco Trench waters and sediments. Earth Planet Sci. Lett. 28, 337–344.
Ritger, S., Carson, B., Suess, E., 1987. Methane-derived authigenic carbonates formed by subduction-induced pore-water expulsion along the Oregon/Washington margin. Geol. Soc. Am. Bull. 98, 147–156.
Rodriguez, N.M., Paull, C.K., Borowski, W.S., 2000. Zonation of authigenic carbonates within gas hydrate-bearing sedimentary sections on the Blake Ridge: offshore southeastern North America. In: In: Paull, C.K., Matsumoto, R., Wallace, P.J., Dillon, W.P. (Eds.), Proceedings of the Ocean Drilling Program, Scientific Results, vol. 164. pp. 301–312.
Scotchman, I.C., 1991. The geochemistry of concretions from the Kimmeridge Clay Formation of southern and eastern England. Sedimentology 38, 79–106.
Selles-Martinez, J., 1996. Concretion morphology, classification and genesis. Earth Sci. Rev. 41, 177–210.
Siegel, D.I., Chamberlain, S.C., Dossert, W.P., 1987. The isotopic and chemical evolution of mineralization in septarian concretions: evidence for paleohydrologic methanogenesis. Geol. Soc. Am. Bull. 99, 385–394.
Sivan, O., Schrag, D.P., Murray, R.W., 2007. Rates of methanogenesis and methanotrophy in deep-sea sediments. Geobiology 5, 141–151.
Slatt, R.M., O'Brien, N.R., 2013. Microfabrics related to porosity development, sedimentary and diagenetic processes, and composition of unconventional resource shale reservoirs as determined by conventional scanning electron microscopy. In: In: Camp, W.K., Diaz, E., Wawak, B. (Eds.), Electron Microscopy of Shale Hydrocarbon Reservoirs. American Association of Petroleum Geologists, Memoir, vol. 102. pp. 37–44.
Smith, J.P., Coffin, R.B., 2014. Methane flux and authigenic carbonate in shallow sediments overlying methane hydrate bearing strata in Alamino Canyon, Gulf of Mexico. Energies 7, 6118–6141.
Snyder, G.T., Dickens, G.R., Tomaru, H., Takeuchi, R., Komatsubara, J., Ishida, Y., Yu, H., 2007. Pore water profiles and authigenic mineralization in shallow marine sediments above the methane-charged system on Umitaka Spur, Japan Sea. Deep Sea Res. Part II Top. Stud. Oceanogr. 54, 1216–1239.
Teichert, B.M.A., Gussone, N., Eisenhauer, A., Bohrmann, G., 2005. Clathrites: archives of near-seafloor pore-fluid evolution ($\delta^{44/40}$Ca, δ^{13}C, δ^{18}O) in gas hydrate environments. Geology 33, 213–216.
Teichert, B.M.A., Johnson, J.E., Solomon, E.A., Giosan, L., Rose, K., Kocheria, M., Connolly, E.C., Torres, M.E., 2014. Composition and origin of authigenic carbonates in the Krishna–Godavari and Mahanadi Basins, eastern continental margin of India. Mar. Petrol. Geol. 58, 438–460.
Thyne, G.D., Boles, J.R., 1989. Isotopic evidence for origin of the Moeraki septarian concretions, New Zealand. J. Sediment. Petrol. 59, 272–279.
Timmers, P.H.A., Welte, C.U., Koehorst, J.J., Plugge, C.M., Jetten, M.S.M., Stams, A.J.M., 2017. Reverse methanogenesis and respiration in methanotrophic archaea. Archaea 2017 22 pages.
Treude, T., Krüger, M., Boetius, A., Jørgensen, B.B., 2005. Environmental control on anaerobic oxidation of methane in the gassy sediments of Eckernförde Bay (German Baltic). Limnol. Oceanogr. 50, 1771–1786.
Veizer, J., 1983. Trace elements and isotopes in sedimentary carbonates. In: Reeder, R.J. (Ed.), Reviews in Mineralogy, 11: Carbonates: Mineralogy and Chemistry. Min. Soc. Amer., Washington, DC, pp. 265–299.
Whiticar, M.J., Faber, E., 1986. Methane oxidation in sediment and water column environments – isotope evidence. Org. Geochem. 10, 759–768.
Woodrow, D.L., Fletcher, F.W., Ahrnsbrak, W.F., 1973. Paleogeography and paleoclimate at the depositional sites of the devonian catskill and old red facies. Geol. Soc. Am. Bull. 84, 3051–3064.
Yoshinaga, M.Y., Holler, T., Goldhammer, T., Wegener, G., Pohlman, J.W., Brunner, B., Kuypers, M.M.M., Hinrichs, K., Elvert, M., 2014. Carbon isotope equilibration during sulphate-limited anaerobic oxidation of methane. Nat. Geosci. 7, 190–194.